

Quantum inductance and negative electrochemical capacitance at finite frequency in a two-plate quantum capacitor

Jian Wang,^{1,*} Baigeng Wang,² and Hong Guo³

¹*Center of Theoretical and Computational Physics and Department of Physics, The University of Hong Kong, Pokfulam Road, Hong Kong, China*

²*Department of Physics, Nanjing University, Nanjing, China*

³*Department of Physics, McGill University, Montreal, Quebec, H3A 2T8, Canada*

(Received 15 January 2007; revised manuscript received 24 February 2007; published 30 April 2007)

We report on theoretical investigations of frequency-dependent quantum capacitance. It is found that at finite frequency, a quantum capacitor can be characterized by a classical RLC circuit with three parameters: a static electrochemical capacitance, a charge relaxation resistance, and a quantum inductance. The quantum inductance is proportional to the characteristic time scale of electron dynamics, and due to its existence, the time-dependent current can accumulate a phase delay and lags behind the applied ac voltage, leading to a negative effective capacitance.

DOI: [10.1103/PhysRevB.75.155336](https://doi.org/10.1103/PhysRevB.75.155336)

PACS number(s): 73.23.-b, 72.10.-d, 73.21.La

Understanding dynamic conductance of quantum coherent conductors is a very important problem in nanoelectronics theory. When two quantum coherent conductors form a double plate “quantum capacitor,” its dynamic conductance $G(\omega)$ is given by the frequency-dependent electrochemical capacitance¹⁻³ $C_\mu(\omega)$, $G(\omega) = -i\omega C_\mu(\omega)$, where ω is the frequency. At low frequency, $C_\mu(\omega)$ can be expanded in frequency, and at the linear order, it is described² by an equivalent classical circuit consisting of a static capacitor C_μ in series with a “charge relaxation resistor” R_q . For a conductor having a single spin-resolved transmission channel, R_q was predicted² to be half the resistance quantum, $R_q = 1/2 G_o$, where $G_o \equiv h/e^2$. The factor $1/2$ in R_q is of quantum origin^{2,4} and has recently been confirmed experimentally.⁵ In the experiment of Gabelli *et al.*,⁵ a submicron two-dimensional electron-gas quantum dot (QD) is capacitively coupled to a gold plate forming a double plate capacitor, where the QD connects to the outside reservoir by a single-channel quantum point contact (QPC). The dynamic conductance $G(\omega)$ is then measured at 1.2 GHz, and the data are well fit to the equivalent circuit characterized by two parameters (C_μ, R_q).

The experiment of Gabelli *et al.*⁵ opened the door for elucidating important and interesting physics of high-frequency quantum transport in meso- and nanoscale devices. An important question is what happens to electrochemical capacitance at higher frequencies beyond the linear ω regime, and, in particular, whether the two-parameter (C_μ, R_q) equivalent circuit is adequate at higher frequencies to describe a quantum capacitor. It is the purpose of this paper to address these issues.

In the following, we report a microscopic theory for high-frequency quantum transport in a two-plate quantum capacitor. Our results show that to characterize its high-frequency dynamic response, one needs—in addition to C_μ and R_q —another quantity L_q having the dimension of inductance. L_q is found to have purely quantum origin and will be named “quantum inductance.” Therefore, the frequency dependent electrochemical capacitance of a quantum capacitor $C_\mu(\omega)$ is equivalent to a classical RLC circuit characterized by three parameters (C_μ, R_q, L_q) at high frequency. Due to L_q , elec-

trons dwell in the neighborhood of the capacitor plates causing a phase delay. At low frequencies, the dynamic response is capacitive-like and voltage lags current. At larger frequencies when $\omega > 1/\sqrt{C_\mu L_q}$, inductive behavior dominates and voltage leads current: in this case, the quantum capacitor gives a negative capacitance value. It is, indeed, surprising that a quantum capacitor can give an inductive dynamic response. For the experimental setup of Ref. 5, we estimate that when $\omega \sim 3$ GHz, the predicted high-frequency effects should be observable.

Let us first work out a simple expression for the frequency-dependent electrochemical capacitance $C_\mu(\omega)$ following the work of Büttiker.² We consider a two-plate capacitor similar to the experiment of Gabelli *et al.*:⁵ a QD, labeled I, and a large metallic electrode, labeled II. Each plate is connected to the outside world through its lead, and a time-dependent bias $v_{1,2}$ is applied across the two leads. We consider small amplitudes of $v_{1,2}$ so as to focus on the linear bias regime. Under the action of such a bias, the two capacitor plates develop their own frequency-dependent electric potential $U_{I,II}(\omega)$. The charge on plate I is equal to the sum of the injected charge and induced charge: $Q_I = Q_I^{inj} + Q_I^{ind}$. In the linear regime, the injected charge is proportional to bias $v_1(\omega)$: $Q_I^{inj} = e^2 D_I(\omega) v_1(\omega)$, where $D_I(\omega)$ is the generalized global density of states (DOS) of plate I at frequency ω . The induced charge, on the other hand, is in general related to a nonlocal Lindhard function² whose calculation is simplified by applying the Thomas-Fermi approximation. Within this approximation, the induced charge is proportional to the induced potential U_I on the plate: $Q_I^{ind} = -e^2 D_I(\omega) U_I$, where the minus sign indicates that the charge is induced. Putting things together, we obtain $Q_I = e^2 D_I(\omega) (v_1 - U_I)$. Clearly, the same charge Q_I can be calculated by the usual electrostatic geometric capacitance C_o : $Q_I = C_o (U_I - U_{II})$. We therefore obtain a relationship: $C_o (U_I - U_{II}) = e^2 D_I(\omega) (v_1 - U_I)$. Applying the same argument to plate II, we similarly obtain $-C_o (U_I - U_{II}) = e^2 D_{II}(\omega) (v_2 - U_{II})$. Finally, the same charge Q_I can also be obtained from the definition of the electrochemical capacitance: $Q_I = C_\mu(\omega) (v_1 - v_2)$. These three relations allow one to derive the following expression for $C_\mu(\omega)$:

$$\frac{e^2}{C_\mu(\omega)} = \frac{e^2}{C_o} + \frac{1}{D_I(\omega)} + \frac{1}{D_{II}(\omega)}. \quad (1)$$

This result resembles the one obtained by Büttiker for the static capacitance.² An important difference is that the frequency-dependent electrochemical capacitance in Eq. (1) is a complex quantity: its real part is a measure of the electrochemical capacitance and its imaginary part is proportional to the frequency-dependent charge relaxation resistance.

To proceed further, we need to calculate the frequency-dependent DOS $D_{I,II}(\omega)$. Following Ref. 4, the generalized local DOS of plate α of the capacitor can be expressed in terms of Green's functions as follows:

$$\frac{dn_\alpha(\omega)}{dE} = \int \frac{dE f - \bar{f}}{2\pi \hbar \omega} [\bar{G}^r \Gamma_\alpha G^a]_{xx}, \quad (2)$$

where the subscript x labels space coordinates and the global DOS is given by

$$D_\alpha(\omega) = \text{Tr} \int \frac{dE f - \bar{f}}{2\pi \hbar \omega} [\bar{G}^r \Gamma_\alpha G^a].$$

In Eq. (2), f is the Fermi function and $\bar{f} \equiv f(E_+)$, with $E_+ \equiv E + \hbar\omega$; $G^{r,a} = G^{r,a}(E)$ is the retarded and/or advanced Green's function at energy E and $\bar{G}^r \equiv G^r(E + \hbar\omega)$; and Γ_α is the linewidth function describing the coupling strength between plate α and its lead. These quantities can be calculated in a straightforward manner when the Hamiltonian of the capacitor model is specified.^{6,7}

For the quantum capacitor of Ref. 5, plate I is a QD and plate II is a metal gate. Since the metal gate has much greater DOS, i.e., $D_{II} \gg D_I$, we can safely neglect the D_{II} term in Eq. (1). For a QD with one energy level E_0 and connected to one lead, its Green's function $G^r = 1/(E - E_0 + i\Gamma_L/2)$, where Γ_L is the linewidth function of the lead. With this Green's function, the frequency-dependent DOS can be easily calculated from Eq. (2), and we obtain

$$D_I(\omega) = \frac{\Gamma_L}{2\pi\hbar\omega(\hbar\omega + i\Gamma_L)} \left[\frac{1}{2} \ln \frac{\Delta^2}{\Delta_+ \Delta_-} - i \left(\arctan \frac{\Delta E - \hbar\omega}{\Gamma_L/2} - \arctan \frac{\Delta E + \hbar\omega}{\Gamma_L/2} \right) \right], \quad (3)$$

where $\Delta = \Delta E^2 + \Gamma_L^2/4$, $\Delta_\pm = (\Delta E \pm \hbar\omega)^2 + \Gamma_L^2/4$, and $\Delta E = E_F - E_0$. At resonance $\Delta E = 0$, we obtain $\text{Re}(D_I(\omega)) = [-x \ln(4x^2 + 1) + 2 \arctan(2x)]/[2\pi\Gamma_L x(x^2 + 1)]$, with $x = \hbar\omega/\Gamma_L$. Hence, $\text{Re}(D_I(\omega))$ is positive for small x and negative for large x , i.e., there is a sign change. A similar behavior is also found for the system away from the resonance. Due to this sign change of $\text{Re}(D_I)$, from Eq. (1), the frequency-dependent electrochemical capacitance $C_R \equiv \text{Re}[C_\mu(\omega)]$ can become negative.

To be more specific, we fix the classical capacitance of QD $C_o = 1$ fF, which is a typical value for QD with an area of $\sim 1 \mu\text{m}^2$. Figure 1 plots $C_R = \text{Re}[C_\mu(\omega)]$ (real part) and $C_I = \text{Im}[C_\mu(\omega)]$ (imaginary part) versus frequency for different values of Γ_L by setting ΔE and temperature to zero. We

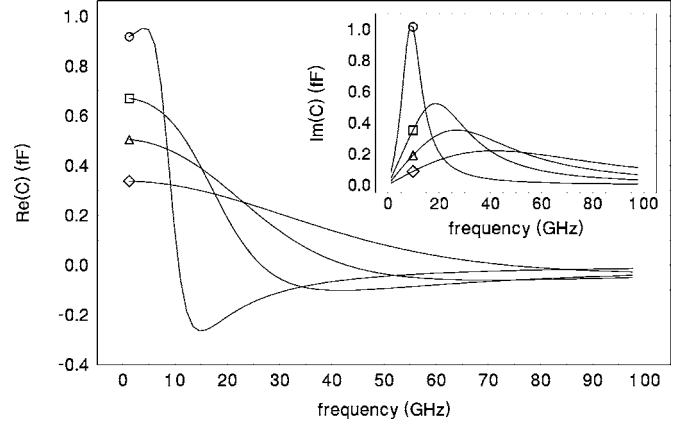


FIG. 1. Frequency-dependent capacitance $C_\mu(\omega)$ versus frequency. Main figure is for C_R and inset is for C_I . Here, $\Gamma_L = 10 \mu\text{eV}$ (for the curve with the open circle), $50 \mu\text{eV}$ (open square), $100 \mu\text{eV}$ (open triangle), and $200 \mu\text{eV}$ (open diamond). Here, $C_o = 1$ fF.

observe that C_R is positive at small frequency and becomes negative at larger frequency. For instance, C_R becomes negative at a “critical” frequency $\omega_c \sim 10$ GHz for $\Gamma_L = 10 \mu\text{eV}$. This critical frequency can be smaller for smaller linewidth function Γ_L . We note that it is not difficult to achieve $\Gamma_L = 10 \mu\text{eV}$ experimentally: in Ref. 8, Γ_L between 1 and $5 \mu\text{eV}$ has been realized. As will be discussed below, the effective Γ_L in the experiment of Ref. 5 is tunable by a gate voltage, so that the critical frequency at which the negative capacitance occurs can be even smaller. The inset of Fig. 1 also shows that as we increase ω , the imaginary part of $C_\mu(\omega)$ starts from zero, reaches a peak value around ω_c , and then decays to zero. The negative capacitance at large frequency can be understood as follows. For a classical capacitor, a charge is accumulated across the capacitor induced by an external voltage. The current and voltage have a fixed phase relationship: the voltage lags behind current with a phase $\pi/2$. For a quantum capacitor at low frequency, there exists a charge relaxation resistance $R_q = h/(2e^2)$ for a single channel plate; therefore, the charge buildup time is the RC time $\tau_{RC} = R_q C_\mu$. For $C_\mu = 1$ fF and $R_q = h/(2e^2)$, this RC time is about $\tau_{RC} = 13$ ps. If the external voltage reverses sign, the charge accumulation will follow the voltage and will also reverse sign in due time. When frequency is low, namely, when $\omega \ll 1/\tau_{RC} = 77$ GHz, the charge buildup follows the ac bias almost instantaneously just like a classical capacitor; thus, the capacitance is positive. When frequency is high, there is a phase difference between the ac bias and the charge buildup. For frequencies comparable to $1/\tau_{RC}$, the charge buildup cannot follow the ac bias; thereby, the capacitance may be negative.

While the above argument explains why it is possible to have negative capacitance, it would indicate a critical frequency to be near 77 GHz. Our results (Fig. 1) show that the calculated ω_c is actually much smaller. This is because there exists a second relevant time scale in the QD, i.e., the dwell time τ_d which is the time spent by electrons inside the QD. The dwell time τ_d can be calculated for specific systems.⁹ Importantly, at resonance, the electrons can dwell inside the

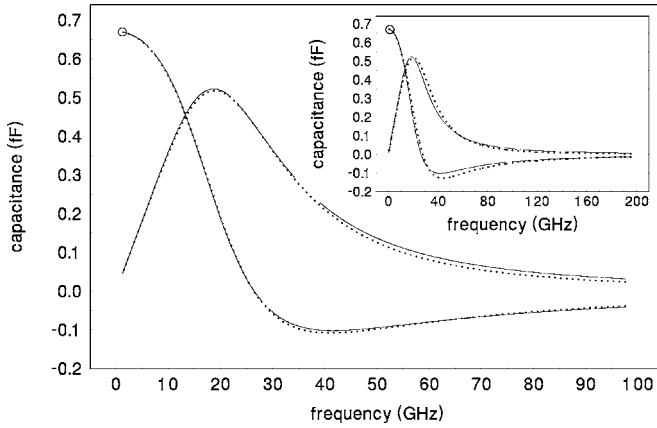


FIG. 2. Comparison of the full quantum capacitance $C_\mu(\omega)$ (solid line) to that obtained by the classical RLC circuit model (dotted line) for $\Gamma_L=50 \mu\text{eV}$. Here, $\text{Re}[C_\mu(\omega)]$ is indicated by open circle. Inset: similar fit but using three constant parameters.

quantum dot for a long time. For instance, for our QD with $\Gamma_L=10 \mu\text{eV}$, we found $\tau_d=260 \text{ ps}$ while $\tau_{RC}=12 \text{ ps}$ (since $C_\mu=0.9 \text{ fF}$). In other words, $\tau_d \gg \tau_{RC}$. Such a τ_d corresponds to a frequency of 4 GHz, much less than $1/\tau_{RC}$. In other words, when ac frequency is greater than $1/\tau_d$, the charges dwell inside the quantum dot and cannot respond to the ac voltage change. As a result, current lags behind voltage, leading to a negative capacitance.¹⁰ This picture agrees very well with the numerical results (Fig. 1).

Having determined the general behavior of $C_\mu(\omega)$ for the quantum capacitor, in the following, we determine how to simulate this quantity using a classical circuit. Expanding Eq. (1) into a Taylor series to second order in ω with the help of Eq. (3) at resonance, we obtain

$$C_\mu(\omega) = C_\mu + i\omega C_\mu^2 \frac{h}{2e^2} - \omega^2 C_\mu^3 \frac{h^2}{4e^4} + \omega^2 C_\mu^2 \frac{h^2}{12\pi\Gamma_L e^2}, \quad (4)$$

where $C_\mu=C_\mu(0)$ on the right-hand side is the static electrochemical capacitance. This result is equivalent to that of a classical RLC circuit as follows. For a classical RLC circuit with capacitance C_μ , resistance R_q , and inductance L_q , the dynamic conductance is

$$G(\omega) = -i\omega C_\mu / (1 - \omega^2 L_q C_\mu - i\omega C_\mu R_q). \quad (5)$$

Expanding this expression in power series of ω , we obtain

$$G(\omega) = -i\omega C_\mu + \omega^2 C_\mu^2 R_q + i\omega^3 C_\mu^3 R_q^2 - i\omega^3 C_\mu^2 L_q. \quad (6)$$

Because for a capacitor $G(\omega)=-i\omega C_\mu(\omega)$, we obtain the result that our quantum capacitance [Eq. (4)] is equivalent to the classical RLC circuit model of Eq. (6). Comparing these two equations, we readily identify $R_q=h/(2e^2)$ —a result first obtained by Büttiker *et al.*² Importantly, another quantity—the equivalent inductance—is identified as $L_q=h^2/(12\pi e^2\Gamma_L)$. In terms of dwell time τ_d and charge relaxation resistance R_q , we obtain

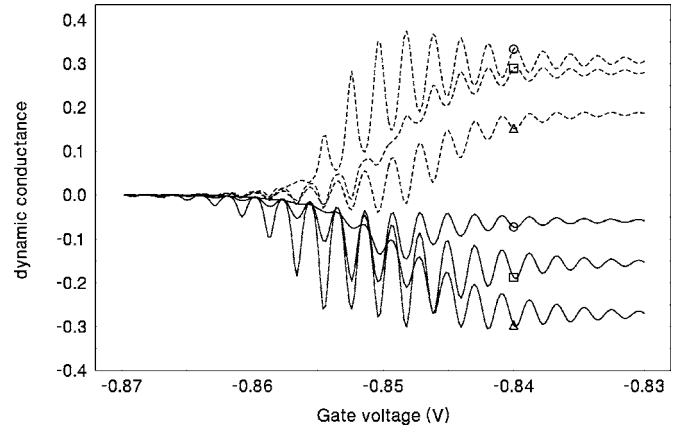


FIG. 3. The dynamic conductance $G(\omega)$ (unit e^2/h) versus gate voltage at different frequencies $\omega=1.2, 3,$ and 5 GHz . Solid line, $\text{Re}[G]/\omega$; dotted line, $\text{Im}[G]/\omega$. Other parameters: $\Delta=500 \text{ mK}$, $\alpha=3000$, $V_0=-0.85$, $\Delta V_0=0.003$, $C_0=4 \text{ fF}$, and temperature 50 mK . For purpose of illustration, we divided $G(\omega)$ by ω . Inset: frequency-dependent R_q (unit h/e^2) vs frequency.

$$L_q = R_q \tau_d / 12, \quad (7)$$

where $\tau_d=4\hbar/\Gamma_L$.

What is the reason that a quantum capacitor at finite frequency needs to be modeled by a classical RLC circuit (instead of a RC circuit)? This is due to the role played by the large dwell time τ_d of the QD. When electrons dwell for long time τ_d inside the QD, the interaction between electrons becomes an important piece of physics which, in our theory, is modeled by the induced self-consistent potential $U_{I,II}$ discussed above. Such an interaction gives rise to the physics of induction, resulting to the quantity L_q of Eq. (7). Indeed, the explicit dependence on τ_d by L_q also confirms the important role played by the dwell time. Because L_q is determined by τ_d , as well as fundamental constants h and e , it is of purely quantum origin and can be called quantum inductance.

Figure 2 compares the fitting of classical RLC circuit [Eq. (5)], with the full quantum result of Eq. (1). They compare very well for the entire range of the frequency—if we treat R_q as a function of ω . Indeed, while R_q has so far been a constant $h/(2e^2)$ as identified through the Taylor expanded equations [Eqs. (4) and (6)], it is actually a function of ω by the more general expression Eq. (5). The inset of Fig. 3 plots the general $R_q=R_q(\omega)$ obtained numerically, and we observe it to be a slowly increasing function of ω . As expected, in the small frequency limit, $R_q(\omega)$ recovers the result of half resistance quantum. For $\Gamma_L=50 \mu\text{eV}$, $R_q(\omega)$ deviates from $h/2e^2$ at about 5 GHz. We have also attempted using three *constant* parameters C_μ , L_q , and $R_q=h/(2e^2)$ into Eq. (5) to compare with the full quantum result of Eq. (1), and a reasonable agreement is obtained (inset of Fig. 2) although not as good as that shown in Fig. 2.

The situation is somewhat different for quantum inductance L_q when the system is *off* resonance [$\Delta E \neq 0$ in Eq. (3)]. In this case, the dwell time τ_d becomes too small to be relevant and another time scale becomes important, namely, the tunneling time τ_t for electrons to go in and/or out of the

QD. The further away E is from E_0 , the longer is τ_r . Hence, in Eq. (7), τ_d should be replaced by τ_r for off resonance. Our result shows that the fitting of full quantum capacitance $C_\mu(\omega)$ using classical parameters C_μ , L_q , and $R_q(\omega)$ is still quite good for off resonance. This further supports the conclusion that the frequency-dependent quantum capacitance can be described by a classical RLC circuit with static electrochemical capacitance, charge relaxation resistance, and a quantum inductance.

Note that our result [Eq. (7)] is obtained using Lorentzian line shape for the Green's function that is a good approximation at low frequency. Now, we compare our result with the high-frequency admittance for a single-channel wire against a macroscopic gate calculated using the Luttinger model.¹³ The low-frequency expansion of gate capacitance is given in the last equation of Ref. 13, from which we can identify L_q to be

$$L_q = \frac{1}{3g^2} C_\mu R_q^2, \quad (8)$$

where the interaction parameter g is related to electrochemical capacitance via

$$C_\mu = \frac{Lg^2}{R_q v_F}, \quad (9)$$

with L the length of the wire and v_F the Fermi velocity. Substituting Eq. (9) into Eq. (8), we have

$$L_q = \frac{L}{3v_F} R_q. \quad (10)$$

We see that if we identify $\tau_d \sim 4L/v_F$, Eqs. (7) and (10) are the same. In another word, a spinless Luttinger liquid has a capacitance with a high-frequency inductance of the same form as in Eq. (7).

Finally, we perform a numerical calculation of the dynamic conductance for the device structure of Ref. 5. In terms of scattering matrix, the DOS of Eq. (2) for a capacitor can be rewritten as^{4,6}

$$D_I(\omega) = i \int \frac{dE}{2\pi \hbar^2 \omega^2} \bar{f} [1 - s_{LL}^\dagger(E_+) s_{LL}(E)], \quad (11)$$

with⁵ $s_{LL}^\dagger(E) = (r - e^{i\phi}) / (1 - r e^{i\phi})$, $\phi = 2\pi E / \Delta$, $r^2 = 1 - T_{QPC}$, and $T_{QPC} = 1 / [1 + \exp(-(V_g + V_0) / \Delta V_0)]$, which is the transmission coefficient of the QPC in the experimental setup.⁵ Figure 3 shows the dynamic conductance $G(\omega)$ vs gate voltage V_g using our theory presented above. When $\omega = 1.2$ GHz (open circle), our results agrees very well¹⁴ with the experimental data of Ref. 5. When $\omega = 3$ GHz (open square), our theory predicts that the imaginary part of $G(\omega)$, which is the electrochemical capacitance, goes to negative. For even larger frequency $\omega = 5$ GHz, the effect is more significant. To understand why one can observe a negative capacitance at small frequency such as 3 GHz, we note that since electron entering the QD has to first pass the QPC,⁵ this QPC serves as a barrier (with an effective barrier height $1/\Gamma$) that is controlled by the gate voltage. At small gate voltage, T_{QPC} is nearly zero and goes to 1 at large V_g . Hence, the effective Γ for small gate voltage is quite large, making ω_c much smaller. Since the experiment of Ref. 5 is performed at $\omega = 1.2$ GHz, we assume that it is not too difficult to push the frequency to 3 GHz so that the effect of quantum inductance can be observed experimentally. Indeed, a single-wall carbon nanotube transistor operated at 2.6 GHz has been demonstrated¹⁵ and measurement of current fluctuation at frequency from 5 to 90 GHz has been reported.¹⁶

In summary, we found that at finite frequency, a quantum capacitor consisting of a quantum dot and a large metal conductor is equivalent to a classical RLC circuit with three basic parameters: a static electrochemical capacitance C_μ , a charge relaxation resistance R_q , and a quantum inductance L_q . It is found that $L_q \sim R_q \tau$, where τ is the characteristic time scale for the quantum dot such as the dwell time τ_d or the tunneling time τ_t . Due to the phase delay by the quantum inductance, the dynamic current can lag behind the applied ac voltage, giving rise to a negative capacitance. Our numerical results show that this effect should be detectable experimentally using the present device technology.

We thank K. Xia for useful discussions. This work is supported by a RGC grant (HKU 7048/06P) from the HKSAR and LuXin Energy Group (J.W.); NSF of China Grants No. 10474034 and No. 60390070 (B.W.); and NSERC of Canada, FQRNT of Québec, and Canadian Institute of Advanced Research (H.G.).

*Electronic address: jianwang@hkusub.hku.hk

¹S. Luryi, Appl. Phys. Lett. **52**, 501 (1998).

²M. Büttiker, J. Phys.: Condens. Matter **5**, 9361 (1993); M. Büttiker, H. Thomas, and A. Pretre, Phys. Lett. A **180**, 364 (1993).

³T. P. Smith, B. B. Goldberg, P. J. Stiles, and M. Heiblum, Phys. Rev. B **32**, 2696 (1985).

⁴S. E. Nigg, R. Lopez, and M. Büttiker, Phys. Rev. Lett. **97**, 206804 (2006).

⁵J. Gabelli *et al.*, Science **313**, 499 (2006).

⁶Z. S. Ma, J. Wang, and H. Guo, Phys. Rev. B **59**, 7575 (1999).

⁷B. G. Wang, J. Wang, and H. Guo, Phys. Rev. Lett. **82**, 398 (1999).

⁸T. Fujisawa *et al.*, Science **282**, 932 (1998).

⁹V. Gasparian, T. Christen, and M. Büttiker, Phys. Rev. A **54**, 4022 (1996).

¹⁰A negative quantum capacitance can arise in the zero-frequency limit but with different origins. See, for instance, Refs. **1**, **11**, and **12**.

¹¹L. Latessa, A. Pecchia, A. Di Carlo, and P. Lugli, Phys. Rev. B **72**, 035455 (2005).

- ¹²Y. D. Wei, X. A. Zhao, B. G. Wang, and J. Wang, *J. Appl. Phys.* **98**, 086103 (2005).
- ¹³Y. M. Blanter, F. W. J. Hekking, and M. Büttiker, *Phys. Rev. Lett.* **81**, 1925 (1998).
- ¹⁴In classical *RC* circuit theory, the convention is writing $v(t) = v_0 \exp(i\omega t)$, while in quantum transport theory, the convention is $v(t) = v_0 \exp(-i\omega t)$. This is responsible for the sign difference between our Fig. 3 and the experimental data of Ref. 5.
- ¹⁵S. D. Li, Z. Yu, S. F. Yen, W. C. Tang, and P. J. Burke, *Nano Lett.* **4**, 753 (2004).
- ¹⁶R. Deblock, E. Onac, L. Gurevich, and L. P. Kouwenhoven, *Science* **301**, 203 (2003).